

James W. Mack¹
M. G. Usha²
Joanna Long³
Robert G. Griffin³
R. J. Wittebort²

¹ Department of Biochemistry
and Molecular Biology,
Howard University
College of Medicine,
Washington, DC

² Department of Chemistry,
University of Louisville,
Louisville, KY

³ Department of Chemistry
and Bitter Magnet Laboratory,
Massachusetts Institute of
Technology, Cambridge, MA

Received 23 March 1999;
accepted 24 May 1999

Backbone Motions in a Crystalline Protein from Field-Dependent ²H-NMR Relaxation and Line-Shape Analysis

Abstract: We have used ²H-nmr to study backbone dynamics of the ²H-labeled, slowly exchanging amide sites of fully hydrated, crystalline hen egg white lysozyme. Order parameters are determined from the residual quadrupole coupling and values increase from $S^2 = 0.85$ at 290 K to $S^2 = 0.94$ at 200 K. Dynamical rates are determined from spin-lattice relaxation at three nmr frequencies (38.8, 61.5, and 76.7 MHz). The approach used here is thus distinct from solution nmr studies where dynamical amplitudes and rates are both determined from relaxation measurements. At temperatures below 250 K, relaxation is independent of the nmr frequency indicating that backbone motions are fast compared to the nmr frequencies. However, as the temperature is increased above 250 K, relaxation is significantly more efficient at the lowest frequency, which shows, in addition, the presence of motions that are slow compared to the nmr frequencies. Using the values of S^2 determined from the residual quadrupole coupling and a model-free relaxation formalism that allows for fast and slow internal motions, we conclude that these slow motions have correlation times in the range of 0.1 to 1.0 μ s and are effectively frozen out at 250 K where fast motions of the amide planes with ~ 15 ps effective correlation times and 9° rms amplitudes dominate relaxation. The fast internal motions increase slightly in amplitude as the temperature rises toward 290 K, but the correlation time, as is also observed in solution nmr studies of RNase H, is approximately constant. These findings are consistent with hypotheses of dynamic glass transitions in hydrated proteins arising from temperature-dependent damping of harmonic modes of motion above the transition point. © 2000 John Wiley & Sons, Inc. Biopoly 53: 9–18, 2000

Keywords: solid-state deuterium nmr spectroscopy; dynamic glass transition; hen egg white lysozyme; crystalline protein; molecular dynamics; spin–lattice relaxation; quadrupole coupling; order parameter; backbone dynamics; damped oscillations; line-shape analysis

INTRODUCTION

The internal dynamics of proteins are of fundamental interest. Correlations of function with dynamics are hypothesized to include the role of fluctuations in facilitating enzyme–substrate engagement,^{1–3} enzymatic activity,^{4–7} the gating of channels or cavities,⁸ and the modulation of protein–protein interactions.^{1,9,10} For example, a direct experimental linkage between function and atomic fluctuations has been observed in ribonuclease A.¹¹ The ability of the enzyme to bind inhibitor is strongly curtailed at temperatures below the protein’s glass transition (~ 200 K) where backbone dynamics are substantially reduced in amplitude. We report here a study of internal dynamics of the exchangeable amides of the globular protein hen egg white lysozyme (HEWL) in hydrated crystalline form using solid-state ^2H -nmr spectroscopy. We report the time scale and amplitude of these motions derived from a combination of T_1 relaxation and lineshape measurements as a function of temperature at three different field strengths. Experiments on crystals of several globular proteins, employing neutron and x-ray scattering and Mössbauer spectroscopy (of heme proteins), have revealed a biphasic behavior in the temperature dependence of their internal conformational flexibility as measured by Debye–Waller or Lamb–Mössbauer factors.^{12–15} The inflection in these factors is commonly regarded as evidence of a dynamic “glass transition.” Here we use solid-state nmr in a complementary way to provide both a quantitative characterization of the frequency spectrum of backbone fluctuations among the slowly exchanging sites of HEWL, and a measure of amplitudes of these fluctuations over a range of temperatures potentially spanning this transition. The amplitudes of all dynamical processes with rates greater than 10^6 s⁻¹ are determined directly from the ^2H -nmr lineshape and rates for these processes, in the range of 10^6 – 10^{12} s⁻¹, are determined by relaxation (T_1) studies at three nmr frequencies (38.8, 61.5, and 76.7 MHz).

While the approach used here for studying internal dynamics does not examine individual sites within the protein backbone, it has several advantageous features when compared with other methods—e.g., solution-state nmr relaxation and molecular dynamics (MD) simulations—that are widely used to study protein dynamics. Molecular dynamics trajectories indicate that the backbone atoms of globular proteins do execute fast motions with rates of the order of 10^{11} s⁻¹.

However, given present technology, MD trajectories are limited to a few nanoseconds for protein systems of ~ 1500 atoms in explicit solvent,^{9,16,17} and rates below 10^9 s⁻¹ can only be inferred qualitatively from ensembles of dynamics. Even these limited trajectories do, however, generally provide accurate predictions of local amide order parameters, even for relatively rare large amplitude jumps, though some care must be exercised in choosing sampling times.¹⁸ Normal mode analysis, a variation on molecular dynamics, can also provide good predictions of order parameters and can even describe low frequency collective motions qualitatively^{19–21}; however, quantitative prediction of correlation times longer than $\sim 10^{-11}$ s is again computationally out of range.

There are several complications in the solution nmr approach to studying internal motions in proteins by relaxation. The internal motions of interest are superimposed on the overall protein tumbling, which is the dominant effect in determining T_1 and other “laboratory frame” relaxation parameters like nuclear Overhauser effects (NOEs) since the tumbling and nmr frequencies are comparable (10^8 – 10^9 s⁻¹). For example, internal dynamical processes occurring at rates slow compared to overall tumbling have no effect on the solution nmr T_1 .²² This insensitivity to slow internal motions is potentially overcome by rotating frame experiments that, in effect, substitute the nutation frequency (10^3 – 10^5 s⁻¹) for the nmr frequency. These experiments are only recently implemented and present additional technical difficulties.²³ A final problem with the interpretation of solution ^{15}N (or ^{13}C) relaxation data is the correct N–H (or C–H) bond length. Since the relaxation time varies with the sixth power of this distance, an error by as little as 0.02 Å has a very significant effect on the order parameters and correlation times derived from relaxation data.

In solid-state spectroscopy no significant overall motion of the molecules occurs on the nmr time scale and relaxation is induced by *internal* motions alone. Further, with the full anisotropic effects of the coupling tensors manifested in the resonance line shapes, the principal frequencies of the spectral patterns give a direct means of determining the order parameter, *independent of relaxation measurements*, that does not exist in solution spectroscopy.²⁴ Since dynamical averaging of the quadrupole coupling tensor results from the presence of motions with rates greater than the quadrupole coupling frequency (the order of 2

Table I Magnitudes of Residual Principal Quadrupolar Coupling Elements $\langle\nu_{ii}\rangle$, and Order Parameters S for the Slowly Exchanging Amide Groups of Crystalline HEWL^a

T (K)	ν_{xx} (kHz)	ν_{yy} (kHz)	ν_{zz} (kHz)	S	S^2	θ_{rms} ($^\circ$)
290	60.5	84.9	145.4	0.92	0.85	13
270	61.5	84.9	146.4	0.93	0.86	12
255	61.5	87.9	149.4	0.95	0.90	10
240	62.5	87.9	150.4	0.96	0.91	9
220	61.5	89.8	151.3	0.96	0.92	9
200	63.5	88.9	152.4	0.97	0.94	8

^a For comparison with other experiments, values of S^2 and $\theta_{\text{rms}} = \langle\theta^2\rangle^{1/2}$ are also tabulated. Experimental uncertainties in the principal frequencies are estimated to be ~ 1 kHz (twice the digital resolution of 0.49 kHz). The corresponding uncertainties in S and S^2 due to experimental uncertainties in ν_{zz} are .01 and .02, respectively.

$\times 10^5 \text{ s}^{-1}$ for deuterium), it is possible to extract information on markedly slower time scales of motion with the solid-state lab frame relaxation experiments than with their solution analogues. Finally, if internal backbone motions in proteins are essentially fast with rates greater than 10^9 s^{-1} , as indicated by MD simulations and solution nmr measurements, then the spin-lattice relaxation of amide sites in a crystalline protein would be independent of the nmr field strength since overall reorientation is absent. Heretofore, few studies of the field-dependence of spin-lattice relaxation have been undertaken for globular proteins in either the solution or solid states. Cole and Torchia observed evidence of field-dependence to ^{15}N relaxation in crystalline ribonuclease.²⁵ However, the differences in T_1 at each of several sites that they measured at two field strengths were comparable to experimental errors. More recently, field-dependence in the relaxation of the membrane-bound peptide gramicidin also has indicated the presence of slow motions.⁸ The solid-state techniques used by these authors and by us in this study complement the newly developed solution $R_{1\rho}$ - R_1 constant relaxation time method of Akke and Palmer.²³

MATERIALS AND METHODS

All exchangeable groups in hen egg white lysozyme (Sigma Chem. Co.) were labeled with deuterium by mild thermal denaturation for 30 min at 48°C in $^2\text{H}_2\text{O}$ at pH = 4.5. Subsequently, the protein was renatured by slow cooling to room temperature, lyophilized to dryness, and recrystallized from protiated solvent at pH 4.5 yielding monoclinic crystals. Previous studies of triclinic and tetragonal crystals of lysozyme have shown that negligible exchange occurs for most amides within these crystals after even as long as 25 days at either pH 4.2 or 7.5.²⁶

^2H -nmr experiments were carried out at three Larmor frequencies—38.8, 61.5, and 76.7 MHz—on homebuilt spectrometers. On each instrument, the carrier frequency

was set at the exact resonance of liquid D_2O (to within digital resolution) so as to guarantee that powder patterns would be symmetric about the carrier. Longitudinal relaxation times were measured using an inversion-recovery scheme employing a $90_x 180_y 90_x$ composite inversion pulse^{27,28} and solid-echo detection. Spectra for line-shape analysis were acquired with the solid-echo pulse sequence.

The following procedure was used to determine T_1 values from the inversion-recovery data. Spectral intensity was taken as the integrated intensity between the two most clearly defined principal values of the powder patterns (ν_{xx} and ν_{yy}). Negligible anisotropy was observed in the relaxation, i.e., all frequencies in the pattern relaxed at the same rate. This intensity vs time data was fit to the standard three-parameter fitting function, $I(t) = A[1 - B \exp(-t/T_1)]$. To verify consistency of T_1 measurements across the three spectrometers, T_1 values were determined on each for a standard sample, crystalline DL-leucine (d_{10}). Due to very rapid internal rotation, the methyl group ^2H T_1 is known to be field independent for this sample. From 288 to 304 K, it was found that the T_1 measurement at 61.5 MHz varied linearly with interpolated values of 29 ms at 291 K and 33 ms at 297 K. These correspond extremely well to the values of 29 ± 0.6 and 34.7 ± 0.5 ms measured on the 38.8 and 76.7 MHz spectrometers at 291 and 297 K respectively. This indicates that systematic errors in the T_1 measurements, arising from differences in the spectrometers, are negligible compared to the protein relaxation times reported here ($T_1 > 300$ ms).

Residual principal frequencies of the powder patterns (Table I) were determined from “single-sided” spectra obtained with a cosine Fourier transform of the echo signal. The ν_{xx} was measured from the peak frequency in the absorption spectrum, and the dominant shoulder, ν_{yy} was determined from the peak frequency in the dispersion signal.

RESULTS

In Figure 1 is shown a temperature profile of the amide ^2H lineshape of lysozyme. The extracted values

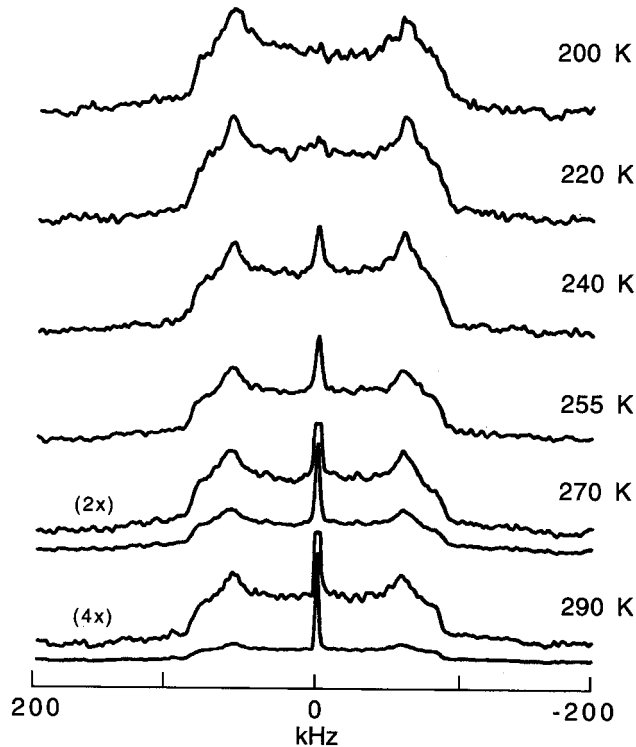


FIGURE 1 Temperature profile of the lineshape of hen egg white lysozyme acquired at 38.8 MHz by transforming the trailing half of the solid-echo signal. Each spectrum is the average of multiple acquisitions with a constant recycle-dealy time of 3 sec. At the lower temperatures S/N degrades as a result of the lengthening of the T_1 relaxation time.

for the residual principal components of the amide quadrupolar coupling tensor—determined from the powder patterns as described in Materials and Methods—and their variation with temperature over the range of 200–290 K are tabulated in Table I. ν_{xx} , ν_{yy} , and ν_{zz} have their largest values at the lowest temperature, showing that dynamical averaging of the coupling tensor is present and increases with increasing temperature. The component ν_{yy} , which lies perpendicular to the peptide plane,²⁹ increases by 5% between 200 and 290 K showing that, on average, the amplitude of amide group dynamics is small. Below 200 K, relaxation times are sufficiently long as to make acquisition of undistorted spectra difficult. Based on earlier findings, ν_{zz} is parallel to the N—H bond.²⁹

For the small amplitude dynamics observed here, the mean-square amplitude $\langle\theta^2\rangle$ and motional order parameter S readily may be related to the residual quadrupole coupling, $\langle\nu_Q\rangle = 4\langle\nu_{zz}\rangle/3$, by³⁰

$$S = 1 - \frac{3}{2} \langle\theta^2\rangle = \frac{\langle\nu_Q\rangle}{\nu_Q} \quad (1)$$

where ν_Q is the coupling for a static amide deuteron. In strongly H-bonded glycy and glutamyl residues ν_Q

is 209–210 kHz.²⁹ We assume that it varies negligibly among the strongly H-bonded amide groups of HEWL and use the value of $\nu_Q = 210$ kHz to calculate the order parameters and mean square amplitudes. The variations of θ and S^2 with temperature are plotted in Figure 2.

While the residual principal components sample only the *amplitude* of peptide dynamics, so long as the dynamics are faster than ν_Q , the relaxation time T_1 depends on both the amplitude and the rate(s) of amide reorientation. Moreover, given dynamics of similar amplitude, processes with rates comparable to the nmr frequency are efficient in affecting relaxation while processes either substantially slower or faster are less important. T_1 values measured at the three nmr frequencies—38.8, 61.5, and 76.7 MHz—and their variation with temperature are shown in Figure 3. At all fields and temperatures, relaxation is observed to be monoexponential, indicating that homogeneous relaxation behavior is being detected. This was confirmed by collecting data with very long relaxation delays (~ 20 -fold greater than T_1) in the inversion-recovery experiments. Owing to the different experimental arrangements used to collect the data at three different spectrometer frequencies, this data is interpolated to a common set of temperatures as

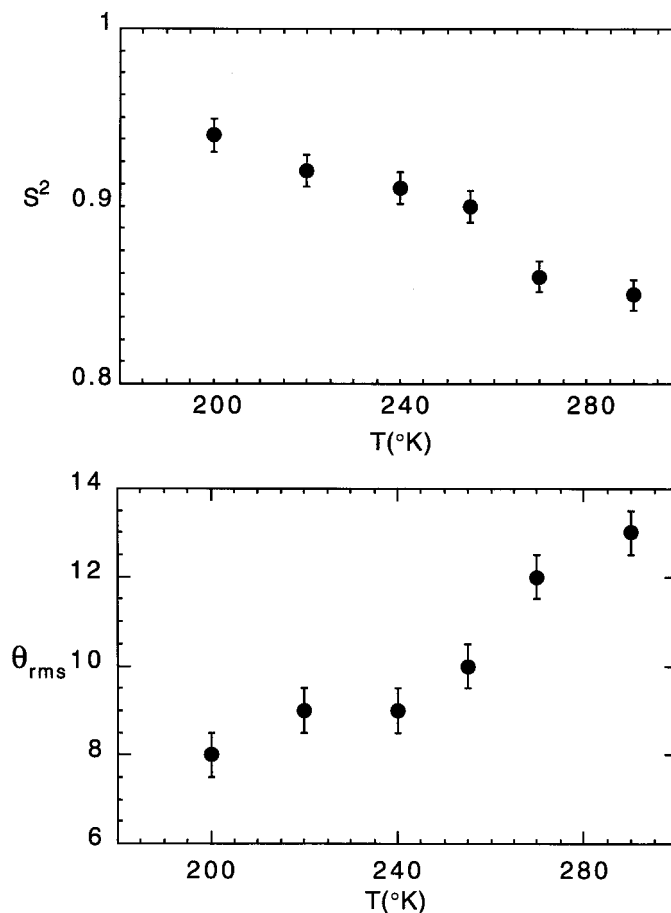


FIGURE 2 Plot of S^2 values (upper graph), derived from the lineshapes as described in the text, vs. temperature. Plot of Θ_{rms} (lower graph), derived from values of S^2 as described in the text, vs. temperature. As temperature decreases from 290°K, the backbone fluctuation amplitudes decrease in an approximately linear fashion.

shown in Table II. Two important qualitative features are apparent from Figure 3 and Table II: (a) Relaxation times decrease substantially as the temperature is raised. (b) Though absent at 250 K, there is marked frequency dependence at the highest temperature, 290 K. For example, the difference between the T_1 s measured at 76.7 MHz (661 ± 35 ms) and 38.8 MHz (420 ± 20 ms) is large compared to the standard deviations in the measurements that, as noted above, are expected to be larger than systematic errors due to the different experimental arrangements. Relaxation is most efficient at the lowest spectrometer frequency.

DISCUSSION

The relatively greater efficiency of relaxation at lower fields above 250 K, together with enhanced efficiency at higher temperatures for any given field, indicates that at least some amide groups experience reorienta-

tion at a slow rate (below the lowest nmr frequency) and that this motion is damped out at low temperatures. Further, these data also suggest that the faster motions may not be appropriately described as being associated with thermally activated diffusion processes, for such would predict *less* efficient relaxation at higher temperature on the fast side of the T_1 minimum.

To discuss more completely the main results, we consider a simple model for amide dynamics that assumes the presence of two motions occurring on different time scales. Both solution ^{15}N -nmr experiments and molecular dynamics simulations of proteins such as RNase H and interleukin-1 β ^{31–35} indicate that almost all amide groups undergo small amplitude motion with order parameters of the order of 0.8 or greater and correlation times in the range of 10–100 ps. Such motions are fast compared to available nmr frequencies ($\omega < 10^9$ Hz), and would result in frequency-independent T_1 relaxation times. Yet

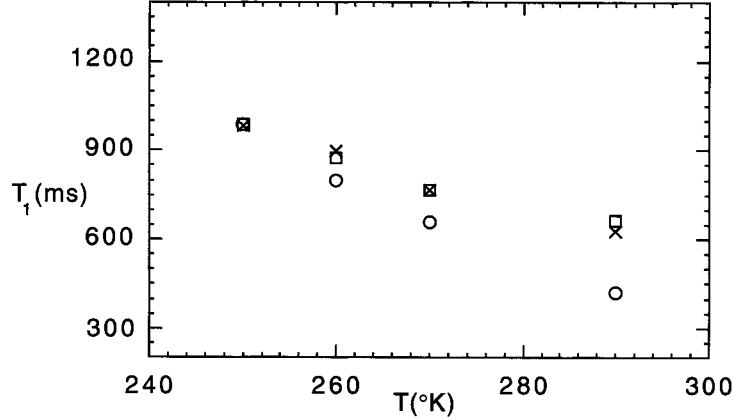


FIGURE 3 Experimental T_1 values versus temperature at three nmr frequencies, 38.8 MHz (\circ), 61.5 MHz (\times) and 76.7 MHz (\square). Below 250°K relaxation is field-independent, but gradually becomes field-dependent above this point. The estimated error in the measurements is $\pm 6\%$ at each spectrometer frequency.

previously a mechanistic model with two internal motions on differing time scales had been introduced to describe solution ^{15}N -nmr relaxation that could not be explained quantitatively by superimposing fast internal motions, with a *single* effective correlation time, on the slow overall diffusive motion of the macromolecule (rotational correlation time $\tau_r \sim 10^{-8}$ s).³¹ In this extended model-free formalism, correlation time τ_f and order parameter S_f are ascribed to the subset of relatively fast internal modes of motion, while τ_s and S_s are analogous parameters for a subset of slower internal motions. It is assumed that the fast and slow motions are uncorrelated to each other and to the overall molecular tumbling. Order parameters S_F and S_S have the usual range of variation²² with the additional constraint that $S^2 = S_F^2 S_S^2$, where S is the total measured order parameter. Using such a correlation function in the limit of a protein fixed in a crystal lattice ($\tau_r \rightarrow \infty$), we obtain the following T_1 expression for the case of quadrupolar relaxation.

$$\frac{1}{T_1} = \frac{3}{40} \omega_Q^2 [J(\omega_0) + 4J(2\omega_0)] \quad (2a)$$

with

$$J(\omega) = (1 - S_F^2) \frac{\tau_F}{1 + \omega^2 \tau_F^2} + S_F^2 (1 - S_S^2) \frac{\tau_S}{1 + \omega^2 \tau_S^2} \quad (2b)$$

When the system is simultaneously in the extreme narrowing limit with regard to the fast internal motion and the slow diffusion limit with respect to the slower internal motion, Eq. (2b) simplifies to

$$J(\omega) = (1 - S_F^2) \tau_F + S_F^2 (1 - S_S^2) \frac{1}{\omega^2 \tau_S} \quad (3)$$

In Figure 4, T_1 calculated from Eqs. (2a) and (2b), is plotted as a function of the slow correlation time τ_S , given a typical value for the fast motion correlation time, $\tau_F = 15$ ps, and selected values of S_F^2 and S_S^2 . It is seen that the inclusion of slow motions decreases T_1 values compared to those generated by fast motions alone and imposes nmr frequency dependence to T_1 for a limited range of correlation times, 10^{-5} s $> \tau_S > 10^{-8}$ s. In this regime relaxation is more

Table II Temperature Dependence of HEWL Amide Deuteron Longitudinal Relaxation Times T_1 at NMR Frequencies of 38.8, 61.5, and 76.7 MHz^a

T (K)	T_1 @ 38.8 MHz (ms)	T_1 @ 61.5 MHz (ms)	T_1 @ 76.7 MHz (ms)
250	988 \pm 60	981 \pm 32	994 \pm 32
260	798 \pm 55	895 \pm 29	874 \pm 42
270	659 \pm 32	768 \pm 25	767 \pm 42
290	420 \pm 20	627 \pm 23	661 \pm 35

^a T_1 values and standard deviations were interpolated to a set of common temperatures using the data shown in Figure 1.

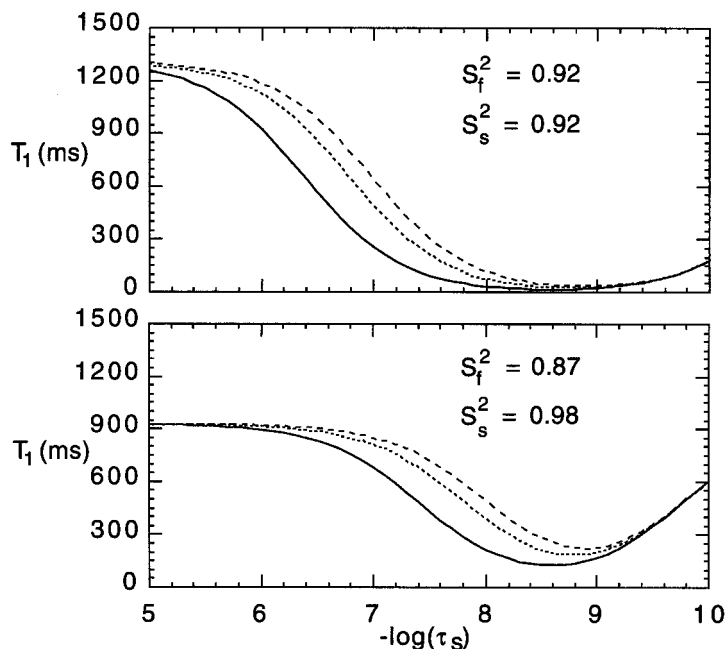


FIGURE 4 Calculated T_1 values vs. $-\log(\tau_s)$ for the two correlation time model. The fast correlation time is fixed at 15 ps. S_s^2 and S_F^2 are constrained so that their product is 0.85. In both figures, the lower, middle, and upper traces correspond to spectrometer frequencies of 38.8, 61.5 and 76.7 MHz, respectively. In the absence of slow motions ($S_s^2 = 1$), $T_1 = 780$ ms for all three spectrometer frequencies.

efficient at lower nmr frequencies. When τ_F becomes sufficiently long, $>10^{-5}$ s, the slow motion no longer affects relaxation and the T_1 is that due to the fast motion alone. Note that for τ_S of the order of the reciprocal of the nmr frequency relaxation rates are very sensitive to the value of S_S^2 as anticipated by Eq. (3). In this regime, for $(1 - S_S^2)$ as small as ~ 0.01 , the second term of Eq. (3) dominates over the first but, as slow motion becomes still more spatially restricted ($S_S^2 \sim 1$), this term becomes negligible; relaxation then is controlled by the faster process. Note that motions outside of this range can be examined in solution nmr using rotating frame (for $\tau_S \geq 10^{-5}$ s)²³ or T_1 , T_2 , and NOE experiments ($\tau_S \leq 10^{-8}$ s).

To fit this model to the relaxation data at any given temperature (Figure 3), we constrain the overall order parameter $S^2 = S_F^2 S_S^2$ to the corresponding value measured from the residual quadrupole coupling (Figure 2). Thus, the two correlation times and S_F^2 (or S_S^2) are chosen to fit best the T_1 s measured at three frequencies. For temperatures from 260 to 290 K, a range of parameter values, listed in Table III, are consistent with the data, i.e., unique values for the three independent parameters are not determined. However, closer examination of the data makes it possible to narrow considerably the range of plausible results. The absence of measurable field-dependence

of the T_1 at 250 K indicates a lower limit of 0.99 for S_S^2 , i.e., the slow motions are largely frozen out. Assuming this, τ_F and S_F^2 then are determined uniquely at this temperature. Then, with the physically reasonable assumption that S_F^2 should decrease with increased temperature (S_F^2 is related to rms displacements of atomic coordinates, which increase with temperature even in the absence of activation barriers), the lower limits of the parameter ranges for τ_F , τ_S , and S_F^2 listed in Table III can be chosen. Thus, in the temperature range of 240–290 K, S_F^2 decreases from 0.91 to 0.87, corresponding to rms amplitudes of 9° – 12° , as determined from Eq. (1). The correlation time τ_F is nearly constant or decreases slightly with reduced temperature. Conversely, the correlation time for the slow motion satisfies the usual expectation for a diffusive process in that τ_S increases as the temperature is lowered, i.e., a slowing of that motion takes place. The apparent absence of these slow motions below 250 K, as judged by T_1 , indicates that their order parameter is large, i.e., the mean square amplitude is quite small, less than a few degrees.

We now compare these results with those obtained by solution nmr. The amide order parameters measured here for HEWL, $S^2 = 0.85$ and $S_F^2 \sim 0.87$ at 290 K compare well with mean solution nmr values of S_F^2 for the great majority of sites in several proteins, as

Table III Correlation Times and Order Parameters for the Fast and Slow Motions of the Strongly H-Bonded Amide Groups of Crystalline HEWL^a

T (K)	τ_F (ps)	τ_S (ns)	S_F^2	S_S^2
290	15–75	100–500	0.87–0.98	0.98–0.87
270	16–95	300–2000	0.88–0.98	0.98–0.88
260	15–80	250–2000	0.89–0.98	0.99–0.90
250	15.5	—	0.90–0.91	1.0–0.99
240	14	—	0.91	1

^a Fast τ_F and slow τ_S correlation times are chosen to best describe the relaxation data (Table II), while S_F^2 and S_S^2 are constrained to the value $S^2 = S_F^2 S_S^2$ determined from the line shape (Table I).

determined from relaxation data (T_1 , T_2 , and NOE); e.g., 0.86 ± 0.02 for staphylococcal nuclease at 298 K,³⁶ $0.82 \pm .05$ for interleukin-1 β at 309 K,³¹ and 0.879 ± 0.002 for RNase H at 285–310 K.^{34,35} Comparable values have been determined from solution studies for the majority of residues of HEWL as well.³⁷ The relative simplicity of the measurement of the residual ²H quadrupole coupling (a first-order property) thus supports the validity of the relaxation approach (a second-order effect) used in solution nmr which depends critically on the choice (1.02 Å) for the equilibrium N—H bond length. The ²H solid-state experiment does have one disadvantage in not being suited to identifying the minority population of sites that do have order parameters dramatically lower than the more typical values of ~ 0.8 . Such minority populations of sites, generally confined to loop regions, with lower than average order parameters, have been found in a few proteins including lysozyme,³⁷ thioredoxin,³⁸ and interleukin-8.³⁹ These would not be discerned in a nonspecific labeling experiment.

The correlation time for fast amide motion determined here, $\tau_F \sim 15$ ps, is also in good agreement with those measured by solution nmr.^{31,35} That τ_F does not lengthen when the temperature is lowered from 290 to 240 K and probably decreases somewhat, extends recent solution nmr studies of RNase H that were limited to a narrower temperature range (285–310 K). It would thus appear that the dominant, fast motion of the amide groups is not thermally activated librational diffusion. Previously it has been suggested that the torsional motion of amide groups in solid polypeptides is due to overdamped oscillatory modes.^{29,40} For such a process, τ_F has the following form²⁹:

$$\tau_F = \frac{\lambda}{2\omega_T^2} \quad (4)$$

Here ω_T and λ are the torsional oscillator frequency and damping constant, respectively. Available evidence indicates that oscillator damping in proteins decreases with decreasing temperature with the largest change at the conformational glass transition, near 200 K, as demarcated by the biphasic character of Debye–Waller factors as a function of temperature in scattering studies of hydrated protein crystals. Below the transition, backbone flexibility becomes quasi-harmonic. The temperature dependence of the apparent τ_F observed here is complementary to this description, even as there is no evident discontinuity in the average backbone order parameter from our measurements.

Finally, both the experiments reported here as well as solution nmr experiments indicate that the protein backbone is subject to motions on much slower time scales than picoseconds, but the solid-state experiments extend the regime of *direct* measurability of these effects considerably vs solution T_1 measurements and comparably to the new $R_{1\rho}$ - R_1 off-resonance rotating frame experiment.²³ The frequency-dependent amide relaxation times observed here, which we attribute to motions that are slow compared to the ²H-nmr frequency, have not been observed previously in a globular protein. Such motions have no effect in the solution nmr relaxation experiment since the correlation times are long, ~ 300 ns or more, compared to the rotational correlation time of the protein. In turn, motions in the 0.5–5 ns timescale identifiable by solution nmr potentially are observed in the solid-state experiments used here, but would impose, at most, very weak field dependence upon T_1 . Additionally, the temperature variation of the principal frequencies of the quadrupolar powder pattern makes it clear that the predominant geometry of backbone motion is well described, on average, by small angle librations about axes connecting successive α C atoms that are nearly coincident with the ν_{xx} axis of the field-gradient tensor, as had been deduced previously.²⁹

SUMMARY

The results obtained here indicate that the dominant motion of amide groups in a fully hydrated crystalline protein at 290 K has a typical correlation time of 15 ns and rms amplitude of 9°–12°. The observation that relaxation is more efficient when measured at a lower nmr frequency indicates the presence of additional slow motions with reciprocal correlation times less than the nmr frequencies, at the majority of amide sites. A simplified model for motion on two time scales,³¹ adapted to a solid protein, indicates that

these slow motions have correlation times in the range of 10^{-7} – 10^{-6} s with substantially smaller amplitudes than the fast motions.

These observations are consistent with the presence of anharmonic character in the backbone modes of the protein at temperatures above 250 K, which can be modeled effectively as arising from damped harmonic modes.²⁹ Below 250 K, the field independence of the relaxation is consistent with the onset of diminished anharmonic character to these modes. This is consistent with observations of a conformational “glass” transition in scattering experiments on hydrated crystalline proteins.⁸ Our experiments complement and extend these observations by characterizing the *dynamic* (kinetic) aspects of conformational flexibility beyond its *static* (equilibrium) qualities as measured by scattering.⁴¹ Earlier ²H-nmr studies of the dynamics of water of hydration in crystalline crambin indicate a broad range of “freezing” for such water molecules—between 250 and 180 K—with effective correlation times reduced to $\sim 10^{-5}$ s below 180 K.¹¹ If, as has been hypothesized, the behavior of water of hydration of proteins has significant effect upon the character of backbone dynamics,⁴² then the observation of a transition in the relaxation behavior of crystalline lysozyme at and below 250 K may be a direct consequence of this. Further, that the nmr results preclude the presence of large amplitude conformational motions about the backbone dihedral angles at any temperature, for the great majority of sites, in spite of the existence of an apparent dynamic transition in terms of time scale, is in agreement with conclusions of molecular dynamics simulations of hydrated proteins in that the transition between anharmonic and quasiharmonic character of backbone fluctuations generally does not involve major dihedral adjustments.⁴³ Further insight into the mechanism of slower modes of motion may now be possible with the practical ability to run dynamics trajectories up to ~ 10 ns.

We wish to thank Dr. Ad Bax for access to the 11.7 T spectrometer and to Mr. Rolf Tschudin for technical assistance. Drs. A. Szabo, D. A. Torchia, and B. R. Brooks participated in useful discussions with us. JWM acknowledges support from NIH/MBRS GM-08016.

REFERENCES

- Brooks, C. L.; Karplus, M.; Pettit, B. M. *Proteins, Advances in Chemical Physics*; John Wiley & Sons: New York, 1988; Vol LXXI.
- Fersht, A. *Enzyme Structure and Mechanism*, 2nd ed.; W. H. Freeman & Co.: New York, 1985.
- Derreumaux, P.; Schlick, T. *Biophys J* 1998, 74, 72–81.
- Steinbach, P. J.; Ansari, A.; Fraunfelder, H.; and others. *Biochemistry* 1991, 30, 3988–4001.
- Zhou, H. X.; Wlodek, S. T.; McCammon, J. A. *Proc Natl Acad Sci USA* 1998, 95, 4280–4283.
- Miller, G. P.; Benkovic, S. J. *Biochemistry* 1998, 37, 6327–6335.
- Zavodszky, P.; Kardos, J.; Svingor, A.; Petsko, G. A. *Proc Natl Acad Sci USA* 1998, 95, 7406–7410.
- North, C. L.; Cross, T. A. *Biochemistry* 1995, 34, 5883–5895.
- Storch, E. M.; Daggett, V. *Biochemistry* 1995, 34, 9682–9693.
- Kay, L. E.; Muhandiram, D. R.; Wolf, G.; Shoelson, S. E.; Forman-Kay, J. D. *Nat Struct Biol* 1998, 5, 156–163.
- Rasmussen, B. F.; Stock, A. M.; Ringe, D.; Petsko, G. A. *Nature* 1992, 357, 423–424.
- Bauminger, E. R.; Cohen, S. G.; Nowik, I.; Ofer, S.; Yariv, J. *Proc Natl Acad Sci USA* 1983, 80, 736–740.
- Doster, W.; Cusak, S.; Petry, W. *Nature* 1989, 337, 754–756.
- Cusak, S.; Doster, W. *Biophys* 1990, 58, 243–251.
- Tilton, R. F.; Dewan, J. C.; Petsko, G. A. *Biochemistry* 1992, 31, 2469–2481.
- Philippopoulos, M.; Lim, E. C. *J Mol Biol* 1995, 254, 771–792.
- Li, A.; Daggett, V. *Protein Eng* 1995, 8, 1117–1128.
- Smith, L. J.; Mark, A. E.; Dobson, C. M.; Van Gunsteren, W. F. *Biochemistry* 1995, 34, 10918–10931.
- Levy, R.; Karplus, M.; Kushick, J.; Perahia, D. *Macromolecules* 1984, 17, 1370–1374.
- Kitao, A.; Hirata, F.; Go, N. *Chem Phys* 1991, 158, 447–472.
- Bruschweiler, R.; Roux, B.; Blackledge, M.; Griesinger, C.; Karplus, M.; Ernst, R. R. *J Am Chem Soc* 1992, 114, 2289–2302.
- Lipari, G.; Szabo, A. *J Am Chem Soc* 1982, 104, 4546–4559.
- Akke, M.; Palmer, A. G. *J Am Chem Soc* 1996, 118, 911–912.
- Torchia, D. A.; Szabo, A. *J Magn Reson* 1985, 64, 135–141.
- Cole, H. B. R.; Torchia, D. A. *Chem Phys* 1991, 158, 271–282.
- Pedersen, T. G.; Sigurskjold, B.; Andersen, K. V.; Kjaer, M.; Poulsen, F.; Dobson, C. M.; Redfield, C. J. *J Mol Biol* 1991, 218, 413–426.
- Levitt, M. H.; Freeman, R. *J Magn Reson* 1979, 33, 473–476.
- Levitt, M. H.; Suter, D.; Ernst, R. R. *J Chem Phys* 1984, 80, 3064–3072.
- Usha, M. G.; Peticolas, W. L.; Wittebort, R. J. *Biochemistry* 1991, 30, 3955–3962.
- Usha, M. G.; Wittebort, R. J. *J Mol Biol* 1989, 208, 669–678.
- Clore, G. M.; Driscoll, P. C.; Wingfield, P. T.; Gronenborn, A. M. *Biochemistry* 1990, 29, 7387–7401.

32. Chandrasekhar, I.; Clore, G. M.; Szabo, A.; Gronenborn, A. M.; Brooks, B. R. *J Mol Biol* 1992, 226, 239–250.
33. Yamasaki, K.; Ogasahara, K.; Yutani, K.; Oobatake, M.; Kanaya, S. *Biochemistry* 1995, 34, 6587–6601.
34. Mandel, A. M.; Akke, M.; Palmer, A. G. *J Mol Biol* 1995, 246, 144–163.
35. Mandel, A. M.; Akke, M.; Palmer, A. G. *Biochemistry* 1996, 35, 16009–16023.
36. Kay, L. E.; Torchia, D. A.; Bax, A. *Biochemistry* 1989, 28, 8972–8979.
37. Buck, M.; Boyd, J.; Redfield, C.; MacKenzie, D. A.; Jeenes, D. J.; Archer, D. B.; Dobson, C. M. *Biochemistry* 1995, 34, 4041.
38. Stone, M. J.; Fairbrother, W. J.; Palmer, A. G.; Reizer, J.; Saier, M. H.; Wright, P. E. *Biochemistry* 1992, 31, 4394–4406.
39. Grasberger, B. L.; Gronenborn, A. M.; Clore, G. M. *J Mol Biol* 1993, 230, 364–372.
40. Usha, M. G.; Speyer, J.; Wittebort, R. J. *Chem Phys* 1991, 158, 487–500.
41. Tang, K. E.; Dill, K. A. *J Biomol Struct Dynam* 1998, 16, 397–411.
42. Steinbach, P. J.; Brooks, B. R. *Proc Natl Acad Sci USA* 1993, 90, 9135–9139.
43. Steinbach, P. J.; Brooks, B. R. *Proc Natl Acad Sci USA* 1996, 93, 55–59.